Efficient Spotlight SAR Raw Signal Simulation of Extended Scenes

Silvia Cimmino, Giorgio Franceschetti, *Life Fellow, IEEE*, Antonio Iodice, *Member, IEEE*, Daniele Riccio, *Senior Member, IEEE*, and Giuseppe Ruello, *Student Member, IEEE*

***Abstract*—Synthetic aperture radar (SAR) raw signal simulation is a powerful tool for designing new sensors, testing processing algorithms, planning missions, and devising inversion algorithms. In this paper, a spotlight SAR raw signal simulator for distributed targets is presented. The proposed procedure is based on a Fourier domain analysis: a proper analytical reformulation of the spotlight SAR raw signal expression is presented. It is shown that this reformulation allows us to design a very efficient simulation scheme that employs fast Fourier transform codes. Accordingly, the computational load is dramatically reduced with respect to a time-domain simulation and this, for the first time, makes spotlight simulation of extended scenes feasible.**

***Index Terms*—Radar, scattering, simulation, spotlight synthetic aperture radar (SAR), synthetic aperture radar (SAR).**

I. Introduction

SYNTHETIC APERTURE radar (SAR) is a powerful remote sensing technique that allows the generation of microwave images of the earth's surface, independently of weather condition and sun illumination. In particular, the SAR spotlight mode [1] is able to obtain a high geometric azimuth resolution by steering the radar antenna beam during the raw data acquisition interval, to always illuminate the same area on the ground. This azimuth steering allows the sensor to obtain a longer synthetic array without reducing the real antenna azimuth size. In the stripmap mode, the same antenna reduction would require an increase in the pulse repetition frequency (PRF), to avoid aliasing and a corresponding reduction in the range swath, to avoid range ambiguity problems [2]; conversely, in the spotlight mode the higher azimuth resolution can be obtained without increasing the pulse repetition frequency, thus avoiding any corresponding increase of the data rate and also avoiding range ambiguity problems. This advantage is paid with an azimuth reduction of the illuminated area and an increase of complexity of data processing needed to obtain the final high resolution image.

Different approaches have been proposed in the last years to process spotlight SAR data [3]–[7]. In order to test processing algorithms, to verify the impact of different system design choices on the final image for different kinds of imaged scenes and finally to help mission planning, a spotlight SAR raw signal simulator is highly desirable. Such a simulator would be really useful only if it meets some stringent requirements: it must account for both SAR system (frequency, chirp bandwidth, antenna dimensions, etc.) and scene (macroscopic height profile, surface roughness, soil dielectric constant, etc.) characteristics; it must be able to deal with extended scenes and not just with a limited number of scattering points; finally, the simulation code must be efficient and time and memory saving. A stripmap SAR raw signal simulator that meets above requirements was presented in [8]–[10]. In this paper, we extend that simulator to include the spotlight mode.

The stripmap simulator of [8]–[10] employs a procedure that consists of two main stages. In the first stage, given the orbit data and the scene geometric and electromagnetic parameters, the scene reflectivity map is evaluated. In the second stage, the SAR raw signal is computed via a superposition integral in which the reflectivity map is weighted by the SAR system two-dimensional (2-D) pulse response (see Section II). This superposition integral is efficiently evaluated in the Fourier domain via fast Fourier transform (FFT) codes. When we move to the spotlight case, the first stage, i.e., the reflectivity map generation, remains conceptually unchanged. With regard to the second stage, the SAR system 2-D pulse response must be properly changed. In addition, the use of the Fourier domain formulation is not straightforward, because the spotlight SAR system transfer function turns out to depend on the azimuth coordinate of the ground point [2]. However, this problem can be overcome as explained in Section II, so that we are still able to use an efficient 2-D FFT-based algorithm in the spotlight case.

To the best of our knowledge, this is the first time that a spotlight SAR raw signal simulator for extended scenes operating in the Fourier-transformed domain is presented. As a matter of fact, up to now only space-domain simulators have been used, such as the point scatterer simulators used to test some processing algorithms (e.g., [7]) and the simulator described in [11]. The advantage of dealing with extended scenes is only paid with the fact that our simulator does not include effects of arbitrary deviations from ideal sensor trajectory. The paper is organized as follows. In Section II, the SAR raw signal for stripmap and spotlight cases is evaluated in both space and frequency domains, in order to explain the method employed to perform the spotlight simulation in the Fourier domain. In Section III, the structure of the spotlight SAR raw signal simulator is described in detail. In Section IV, some simulation results are presented and discussed, in order to assess the effectiveness of the simulator. Finally, in Section V some concluding remarks are reported.

Manuscript received September 25, 2002; revised May 20, 2003.

S. Cimmino is with Wide Sensing (WISE), 80078 Pozzuoli (NA), Italy (e-mail: s.cimmino@wise-widesensing.it).

G. Franceschetti, A. Iodice, D.Riccio, and G. Ruello are with the Dipartimento di Ingegneria Elettronica e delle Telecomunicazioni, Università di Napoli "Federico II," 80125 Napoli, Italy (e-mail: gfrance@unina.it; iodice@unina.it; daniele.riccio@unina.it; ruello@unina.it).

Digital Object Identifier 10.1109/TGRS.2003.815239

II. SAR Raw Signal Evaluation

In this section, we evaluate the SAR raw signal for both the stripmap and the spotlight modes and both in time and frequency domains, in order to devise a method to extend the efficient frequency domain approach used in the stripmap simulator to the spotlight case. We perform here a continuous time analysis and defer to Section III considerations regarding PRF and sampling frequency problems.

We first evaluate the SAR raw signal for the stripmap mode. Chirp modulation (i.e., linear FM) of the transmitted pulse is assumed. We get the following expression for the SAR raw signal (after heterodyne, i.e., downconversion to baseband) [2], [8]–[10] (see also Fig. 1):

$$h_{\text{strip}}(x',r') = \iint \gamma(x,r)\exp\left[-j\frac{4\pi}{\lambda}\Delta R\right] \cdot \exp\left[-j\frac{4\pi}{\lambda}\frac{\frac{\Delta f}{f}}{c\tau}(r'-r-\Delta R)^2\right] \cdot w^2\left(\frac{x'-x}{X}\right)\text{rect}\left[\frac{(r'-r-\Delta R)}{\frac{c\tau}{2}}\right]dxdr \tag{2.1}$$

with

$$\Delta R = R - r = \sqrt{r^2+(x'-x)^2} - r. \tag{2.2}$$

In (2.1) and (2.2), we have the following.

- x, r, ϑ — coordinates in the cylindrical coordinate system whose x axis is the sensor line of flight;
- $A \equiv (x', 0, 0)$ — antenna position;
- $\gamma(x,r)$ — scene reflectivity pattern, including the phase factor $\exp[-j(4\pi/\lambda)r]$;
- λ, f — carrier wavelength and frequency of the transmitted signal, respectively;
- R — distance from A to the generic point $(x, r, \vartheta(x,r))$ of the scene;
- $\vartheta = \vartheta(x,r)$ — soil surface equation in cylindrical coordinates, which allows calculation of the local look angle from the range and azimuth position of the ground point; it can be derived from knowledge of the sensor line of flight and of the scene topography (see [8]–[10]);
- R_0 — distance from the line of flight to the center of the scene;
- Δf — chirp bandwidth;
- c — speed of light;
- τ — pulse duration time;
- $w(\cdot)$ — azimuth illumination diagram of the real antenna over the ground;
- $X = \lambda R_0/L$ — real antenna azimuth footprint; we assume that $w(\cdot)$ is negligible when the absolute value of its argument is larger than 1/2;
- L — azimuth dimension of the real antenna;
- $\text{rect}[t/T]$ — standard rectangular window function, i.e., $\text{rect}[t/T] = 1$ if $|t| \le T/2$; otherwise $\text{rect}[t/T] = 0$;
- r' — $c/2$ times the time elapsed from the pulse transmission.

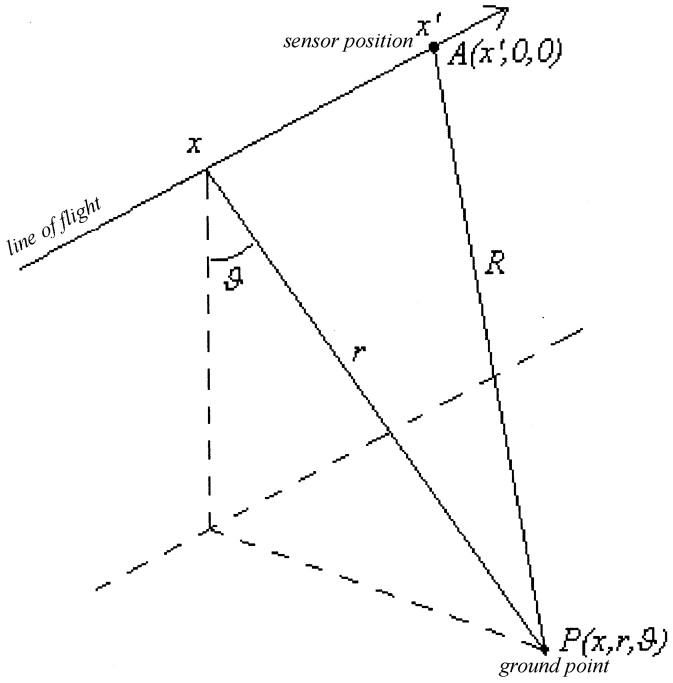

Fig. 1. Geometry of the problem.

TABLE I
Main SAR System Data Used in the Simulation Runs

Platform height (h)	775 km
Platform velocity (v)	6.69 km/s
Look angle (ϑ)	23 degrees
Azimuth antenna dimension (L)	15.0 m
Range antenna dimension	2 m
Carrier frequency (f)	5.3 GHz
Pulse duration (τ)	55 μs
Pulse bandwidth (Δf)	70 MHz
Sampling frequency (f_s)	100 MHz
Pulse repetition frequency (PRF)	900 Hz
Spotlight mode gain (X_1/X)	3

The Fourier transform (FT) of (2.1) can be performed by using the stationary phase method, thus obtaining the following raw signal expression in the frequency domain[1] [2], [8]–[10]:

$$H_{\text{strip}}(\xi,\eta) = \iint \gamma(x,r)G_{\text{strip}}(\xi,\eta;r) \cdot \exp[-j\xi x]\exp[-j\eta r]\,dxdr \tag{2.3}$$

where

$$G_{\text{strip}}(\xi,\eta;r) = \exp\left[-j\frac{\eta^2}{4b}\right]\exp\left[-j\frac{\xi^2\left(\frac{r}{R_0}\right)}{4a\left(1+\frac{\eta\lambda}{(4\pi)}\right)}\right] \cdot \text{rect}\left[\frac{\eta}{\frac{2bc\tau}{2}}\right] w^2\left(\frac{\xi}{2aX}\right) \tag{2.4}$$

[1]In this expression, as well as in (2.7) and (2.11), nonessential multiplicative constants are ignored.

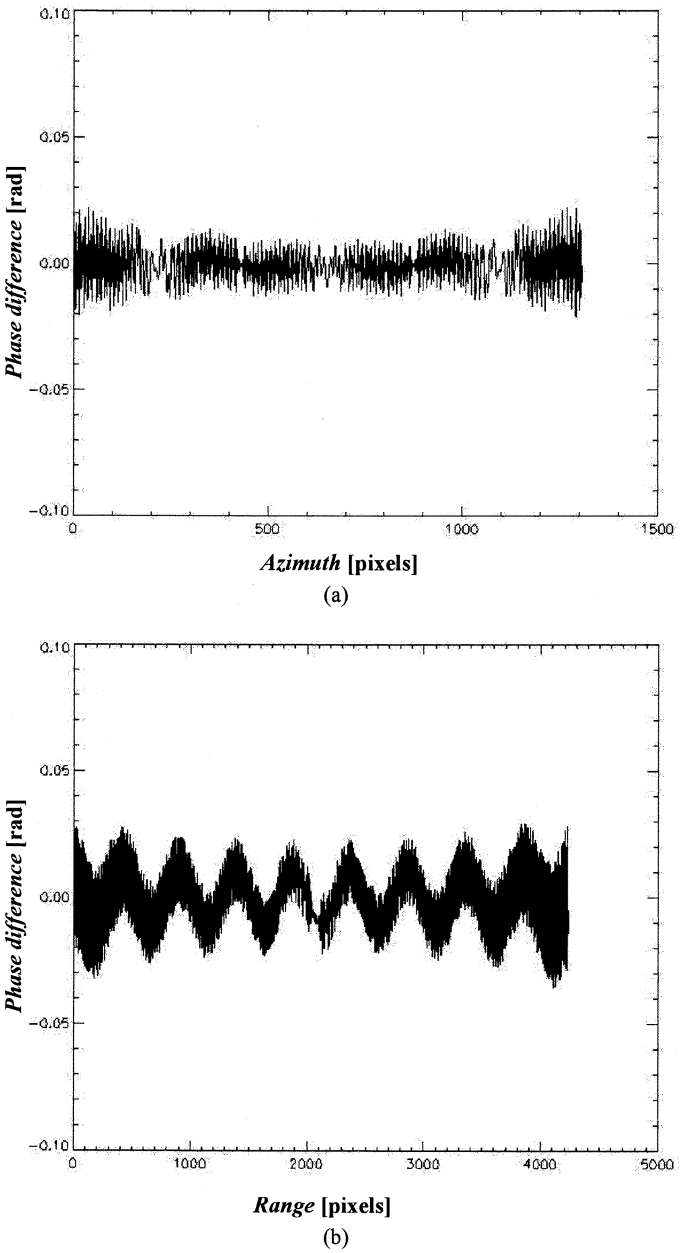

Fig. 2. Difference between the phase of the raw signal simulated by using the proposed approach and the phase of the raw signal obtained by time-domain simulation. (a) Azimuth cut. (b) Range cut. The scattering point is placed in the center of the illuminated scene.

is the space-variant SAR system transfer function (STF) in the stripmap mode and

$$a = \frac{2\pi}{\lambda R_0} \quad b = \frac{4\pi}{\lambda}\frac{\frac{\Delta f}{f}}{c\tau}.$$

By exploiting the particular form of the r dependence in (2.4), (2.3) can be rewritten as [2], [8]

$$H_{\text{strip}}(\xi,\eta) = G_{0\text{strip}}(\xi,\eta)\Gamma(\xi,\eta\Omega(\xi)+\mu(\xi)) \tag{2.5}$$

in which $\Gamma(\xi,\eta)$ is the FT of $\gamma(x,r)$, $G_{0\text{strip}}(\xi,\eta) = G_{\text{strip}}(\xi,\eta;r = R_0)$, and $\Omega(\xi)$ and $\mu(\xi)$ account for the space-variant characteristics of the SAR STF (i.e., the focus depth variation). Their full expressions are

$$\mu(\xi) = \frac{\xi^2}{4aR_0} \quad \Omega(\xi) = 1 - \frac{\xi^2}{4aR_0}\frac{\lambda}{4\pi}.$$

The range migration effect is automatically taken into account by the 2-D formulation of (2.3)–(2.5).

Equation (2.5) suggests that the stripmap SAR raw signal simulation can be performed via the following steps:

- generation of the scene reflectivity pattern $\gamma(x,r)$;
- 2-D FFT of the reflectivity pattern, to obtain $\Gamma(\xi,\eta)$;
- interpolation in the Fourier domain, to obtain the desired values $\Gamma(\xi,\eta\Omega(\xi)+\mu(\xi))$ from the available ones $\Gamma(\xi,\eta)$;
- multiplication by $G_{0\text{strip}}(\xi,\eta)$, to obtain the FT H_{strip} of the raw signal;
- 2-D inverse FFT, to finally obtain the SAR raw signal $h_{\text{strip}}(x',r')$.

This is actually the method employed in the stripmap SAR raw signal simulator presented in [8]–[10]. Note that 2-D Fourier transform and subsequent Fourier domain interpolation are only conceptually two separated steps. In practice, if $\Omega \cong 1$ interpolation can be precisely and efficiently performed by multiplying the azimuth-transformed reflectivity by a linear (with respect to r) phase exponential before range-transforming it. If Ω cannot be approximated by unity, 2-D transform and interpolation can be performed with high accuracy by using a chirp scaling algorithm [12].

Let us now move to the spotlight mode. In this case, the SAR raw signal can be expressed as follows [2]:

$$\begin{aligned} h_{\text{spot}}(x',r') = \iint & \gamma(x,r)\exp\left[-j\frac{4\pi}{\lambda}\Delta R\right] \\ & \cdot\exp\left[-j\frac{4\pi}{\lambda}\frac{\frac{\Delta f}{f}}{c\tau}(r'-r-\Delta R)^2\right] w^2\left(\frac{x}{X}\right) \\ & \cdot\operatorname{rect}\left[\frac{x'}{X_1}\right]\operatorname{rect}\left[\frac{(r'-r-\Delta R)}{\frac{c\tau}{2}}\right] dxdr \end{aligned} \tag{2.6}$$

where X_1 is the length of the trajectory flight portion used to acquire the raw data. Note that, due to the different acquisition geometry, in the spotlight case the antenna azimuth pattern $w(\cdot)$ depends on x and not on the difference $x-x'$ as in the stripmap case; in addition, (2.6) includes a $\operatorname{rect}[\cdot]$ function of width X_1, accounting for the finite length of the trajectory flight portion used to acquire the raw data.

The FT of (2.6) can be performed by using again the stationary phase method, thus obtaining the following raw signal expression in the frequency domain [2]:

$$\begin{aligned} H_{\text{spot}}(\xi,\eta) = \iint & \gamma(x,r)w^2\left(\frac{x}{X}\right)G_{\text{spot}}(\xi,\eta;x,r) \\ & \cdot\exp[-j\xi x]\exp[-j\eta r]dxdr \end{aligned} \tag{2.7}$$

where

$$G_{\text{spot}}(\xi,\eta;x,r)=\exp\left[-j\frac{\eta^2}{4b}\right]\exp\left[-j\frac{\xi^2\left(\frac{r}{R_0}\right)}{4a\left(1+\frac{\eta\lambda}{(4\pi)}\right)}\right]\cdot\text{rect}\left[\frac{\eta}{\frac{2bc\tau}{2}}\right]\text{rect}\left(\frac{\xi-2ax}{2aX_1}\right) \quad (2.8)$$

is the space-variant SAR STF in the spotlight mode.[2] Equations (2.7) and (2.8) are very interesting, since they show [see the last rect term in (2.8)] that the FT of the raw signal of a point scatterer placed in (x,r) is centered around an azimuth frequency dependent on x and its azimuth bandwidth is increased by a factor X_1/X with respect to the stripmap case, so that the azimuth resolution is improved by the same factor. However, (2.7) and (2.8) are not useful if one wants to perform a simulation in the Fourier domain. In fact, due to the x dependence of the spotlight SAR STF via the last $\text{rect}[\cdot]$ function in (2.8), these equations cannot be cast in a form similar to that of (2.5). This problem can be solved by rewriting (2.6) as

$$h_{\text{spot}}(x',r')=\text{rect}\left[\frac{x'}{X_1}\right]\tilde{h}_{\text{spot}}(x',r') \quad (2.9)$$

with

$$\tilde{h}_{\text{spot}}(x',r')=\iint\gamma(x,r)\exp\left[-j\frac{4\pi}{\lambda}\Delta R\right]\cdot\exp\left[-j\frac{4\pi}{\lambda}\frac{\frac{\Delta f}{f}}{c\tau}(r'-r-\Delta R)^2\right]w^2\left(\frac{x}{X}\right)\cdot\text{rect}\left[\frac{x'-x}{X+X_1}\right]\text{rect}\left[\frac{(r'-r-\Delta R)}{\frac{c\tau}{2}}\right]dxdr. \quad (2.10)$$

Note that inclusion of $\text{rect}[(x'-x)/(X+X_1)]$ does not alter the value of (2.9) and (2.10), because this factor is equal to one if both $\text{rect}[x'/X_1]$ and $w^2(x/X)$ are not null.

Equation (2.9), even if very simple, is essential for modeling the spotlight simulator as a stripmap one. In fact, (2.10) is now formally very similar to (2.1) and can be similarly treated. Accordingly, by using the stationary phase method we obtain the FT of $\tilde{h}_{\text{spot}}(x',r')$

$$\tilde{H}_{\text{spot}}(\xi,\eta)=\iint\gamma(x,r)w^2\left(\frac{x}{X}\right)\tilde{G}_{\text{spot}}(\xi,\eta;r)\cdot\exp[-j\xi x]\exp[-j\eta r]dxdr \quad (2.11)$$

where

$$\tilde{G}_{\text{spot}}(\xi,\eta;r)=\exp\left[-j\frac{\eta^2}{4b}\right]\exp\left[-j\frac{\xi^2\left(\frac{r}{R_0}\right)}{4a\left(1+\frac{\eta\lambda}{(4\pi)}\right)}\right]\cdot\text{rect}\left[\frac{\eta}{\frac{2bc\tau}{2}}\right]\text{rect}\left(\frac{\xi}{2a(X+X_1)}\right). \quad (2.12)$$

[2]Equation (2.8) holds for $X_1^4 < R_0^3\lambda$ and is here used only for the sake of simplicity. This condition is usually, but not always, met by actual spotlight SAR systems. In order to account for a larger variation of the observation angle during the acquisition time, a more precise (but more involved) expression is available [2]. Considerations reported in this paper also apply to this more precise expression.

Equation (2.12) is identical to (2.4), except for the last "rect" function that replaces the azimuth antenna pattern, so that (2.11) can be recast in the form

$$\tilde{H}_{\text{spot}}(\xi,\eta)=\tilde{G}_{0\text{spot}}(\xi,\eta)\bar{\Gamma}(\xi,\eta\Omega(\xi)+\mu(\xi)) \quad (2.13)$$

in which $\bar{\Gamma}(\xi,\eta)$ is the FT of $\gamma(x,r)w^2(x/X)$ and $\tilde{G}_{0\text{spot}}(\xi,\eta)=\tilde{G}_{\text{spot}}(\xi,\eta;r=R_0)$. Note that the azimuth bandwidth of $\tilde{h}_{\text{spot}}(x',r')$, and hence (at least approximately) of the overall raw signal bandwidth, is increased by a factor $1+X_1/X$ with respect to the stripmap case.

Equations (2.9) and (2.13) suggest that the spotlight SAR raw signal simulation can be performed via the following steps:

- generation of the scene reflectivity pattern, including the antenna pattern: $\gamma(x,r)w^2(x/X)$;
- 2-D FFT of the reflectivity pattern, to obtain $\bar{\Gamma}(\xi,\eta)$;
- interpolation in the Fourier domain, to obtain the desired values $\bar{\Gamma}(\xi,\eta\Omega(\xi)+\mu(\xi))$ from the available ones $\bar{\Gamma}(\xi,\eta)$;
- multiplication by $\tilde{G}_{0\text{spot}}(\xi,\eta)$, so obtaining the FT $\tilde{H}_{\text{spot}}(\xi,\eta)$ of $\tilde{h}_{\text{spot}}(x',r')$;
- 2-D inverse FFT, to obtain $\tilde{h}_{\text{spot}}(x',r')$;
- multiplication by $\text{rect}[x'/X_1]$, in order to finally obtain the spotlight raw signal $h_{\text{spot}}(x',r')$.

This is the method employed in the simulator that we here propose, described in the next section. This procedure has two main advantages: first of all, use is made of efficient FFT codes, thus reducing the computational load with respect to a time-domain simulation; in addition, the procedure is analogous to the one used in the existing stripmap simulator, so that most of the algorithms employed in that simulator can be reused after minor changes.

It must be noted that the presented procedure assumes a straight line flight path. This is usually a good approximation for a few kilometers portion of the elliptical orbit of a spaceborne sensor. Conversely, in the case of airborne sensors appreciable deviations from the ideal trajectory may occur: effects of these deviations are not included in our simulator and arbitrary deviations cannot be accounted for by any Fourier domain simulator. However, the effect of some particular kinds of deviations from ideal trajectory (e.g., sinusoidal deviations, or sufficiently smooth deviations) can be accounted for by properly modifying the system transfer function, according to the guidelines provided in [13]. This approach would be useful for instance to identify cases that require motion compensation. However, if a motion compensation algorithm must be tested, use of a point target simulator is sufficient and more appropriate.

Finally, it can be shown that the effect of a squinted acquisition geometry could be included in our formulation by adding a proper shift to the last "rect" function of (2.12) and appropriately modifying the simulation of the reflectivity pattern. The application of the proposed simulation scheme to the case of squinted geometry is certainly interesting, because in this case it is known that spotlight processing algorithms often degrade. However, full analysis and assessment of the simulator behavior for squinted geometries deserve an "ad hoc" discussion that would be beyond the scope of this paper. Accordingly, in the following we consider a nonsquinted geometry and defer the complete analysis of squinted geometries to future work.

III. Spotlight Simulator

Analogously to the stripmap simulator of [8]–[10], the proposed spotlight simulator employs a procedure that consists of two main stages. In the first stage, given the orbit data and the scene geometric and electromagnetic parameters, the scene reflectivity map is evaluated. In the second stage, the SAR raw signal is computed via a superposition integral in which the reflectivity map is weighted by the SAR system 2-D pulse response. With regard to the first stage, the imaged scene surface profile is approximated by rectangular planar facets, to whom a random small scale roughness is superimposed. The field backscattered by each facet is evaluated as in [8] by taking into account facet slope, roughness and electromagnetic parameters, transmitting and receiving polarizations and incidence angle, so that a reflectivity map is obtained. A ground range to slant range projection ensures that foreshortening and layover effects are taken into account [8], whereas a recursive ray-tracing procedure identifies the shadowed facets [8]. Details on this first stage of the simulation procedure can be found in [8]–[10]. However, in the spotlight case some more considerations are needed on the choice of facets' dimensions and on the evaluation of the incidence angle.

The facets' linear dimensions can be chosen much larger than wavelength. However they must be small enough to allow that the corresponding discretized reflectivity map accurately approximates the true reflectivity map over a bandwidth larger than the one of $\tilde{G}_{\rm spot}$, i.e., larger than $2a(X+X_1)$ and $bc\tau$ in the azimuth and range directions, respectively [see (2.12)]. Accordingly, the facet's range size must be smaller than the system range resolution: we set this size equal to the final range pixel spacing $c/(2f_s)$, where f_s is the received signal sampling frequency. And the facet's azimuth size must be smaller than $2\pi/[2a(X+X_1)]$, i.e., than $L/2/(1+X_1/X)$: we set this size equal to $v/\mathrm{PRF}/(1+X_1/X)$, where v is the sensor velocity, PRF is the system pulse repetition frequency and v/PRF must not be greater than $L/2$.

With regard to the incidence angle on each single facet, it obviously depends on facet position and slope and also on the sensor position, and hence it varies during the integration time. This change is of course stronger in the spotlight than in the stripmap mode. However, even in the spotlight case the change in the incidence angle during the acquisition time is usually quite small, in fact usually $X_1 \ll R_0$. Since the reflectivity function of most targets is slowly varying with the incidence angle, in order to evaluate the facet reflectivity (and *only* to this aim) we can assume that the incidence direction is fixed and coincident with the range direction $\hat{r}$ during the whole integration time. In other words, we assume $\gamma(x,r,x'-x) \cong \gamma(x,r)$.

Let us now move to analyze the second main stage of the simulation procedure, i.e., the evaluation of the raw signal via the superposition integral, (2.6). This evaluation is performed according to the scheme outlined at the end of the previous section. Of course, in practice all the computations are performed in discrete time. The reflectivity map $\gamma(x,r)$, sampled at spatial frequencies $2f_s/c$ in range and $(1+X_1/X)\mathrm{PRF}/v$ in azimuth, is Fourier-transformed via a 2-D FFT algorithm, the resulting transformed map is properly interpolated (see Section II) and then multiplied by $\tilde{G}_{\rm spot}$ and finally an inverse FFT is performed, to obtain $\tilde{h}_{\rm spot}(x',r')$, still sampled at spatial frequencies $2f_s/c$ in range and $(1+X_1/X)\mathrm{PRF}/v$ in azimuth (so that aliasing is avoided). This modified raw signal has an overall length equal to X_1+X (in fact, all FFT processing is performed over signals whose azimuth length is the sum of reflectivity and pulse response lengths). However, its samples outside the central interval of length X_1 are finally set to zero. This last operation corresponds to the multiplication by $\mathrm{rect}[x'/X_1]$, mentioned as the last step of the procedure outlined in Section II and allows us to obtain the spotlight raw signal $h_{\rm spot}(x',r')$. At this point the simulated raw signal turns out to be azimuth sampled at a frequency that corresponds to a PRF equal to $g=(1+X_1/X)$ times the actual one. A decimation operation is then needed to recover the raw signal corresponding to the actual PRF.

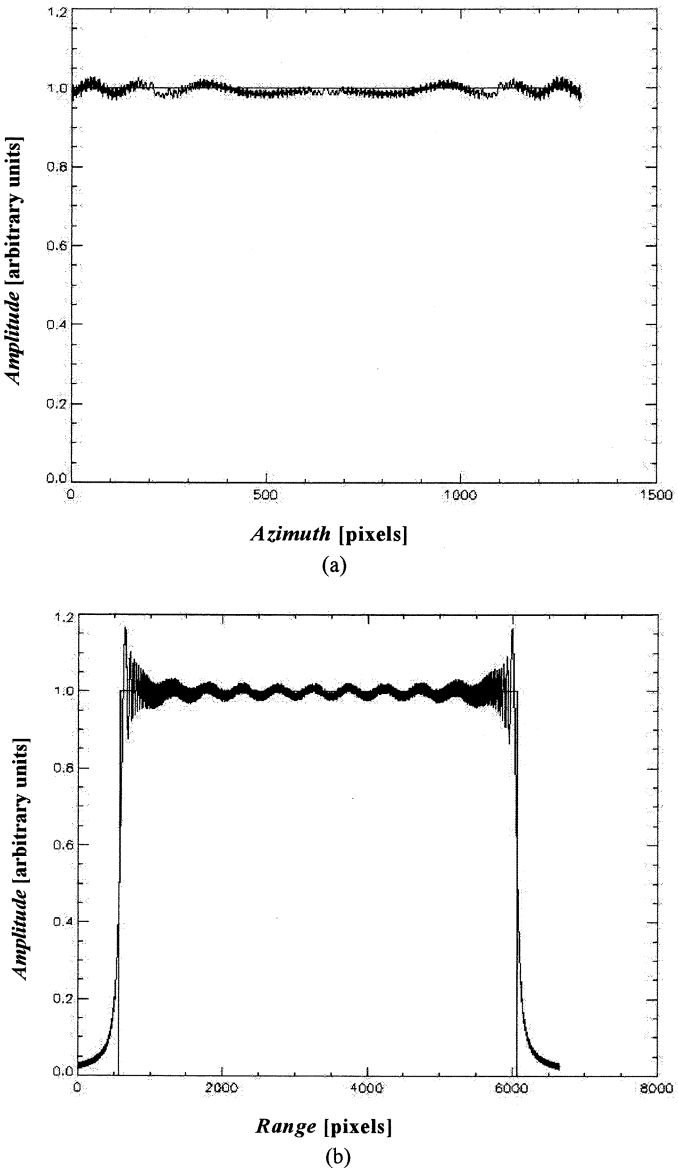

Fig. 3. Amplitudes of the raw signals simulated by using the proposed approach (oscillating curve) and obtained by time-domain simulation (straight line). (a) Azimuth cut. (b) Range cut. The scattering point is placed in the center of the illuminated scene.

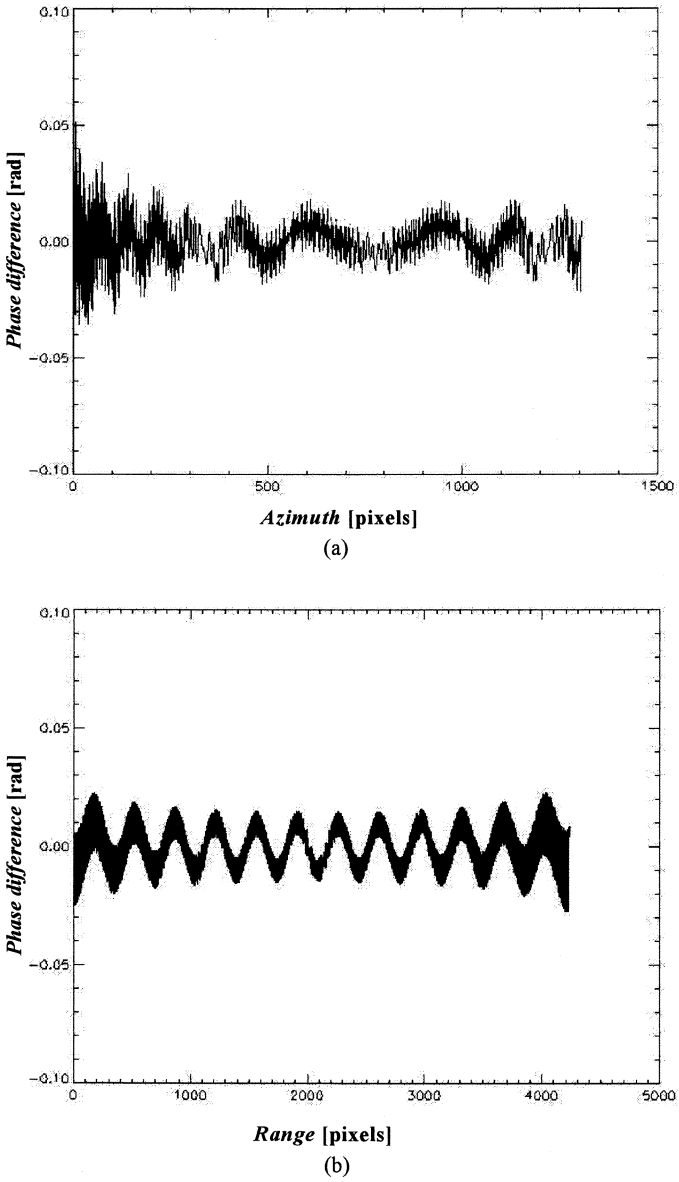

Fig. 4. Difference between the phase of the raw signal simulated by using the proposed approach and the phase of the raw signal obtained by time-domain simulation. (a) Azimuth cut. (b) Range cut. The scattering point is placed near the azimuth border of the illuminated scene.

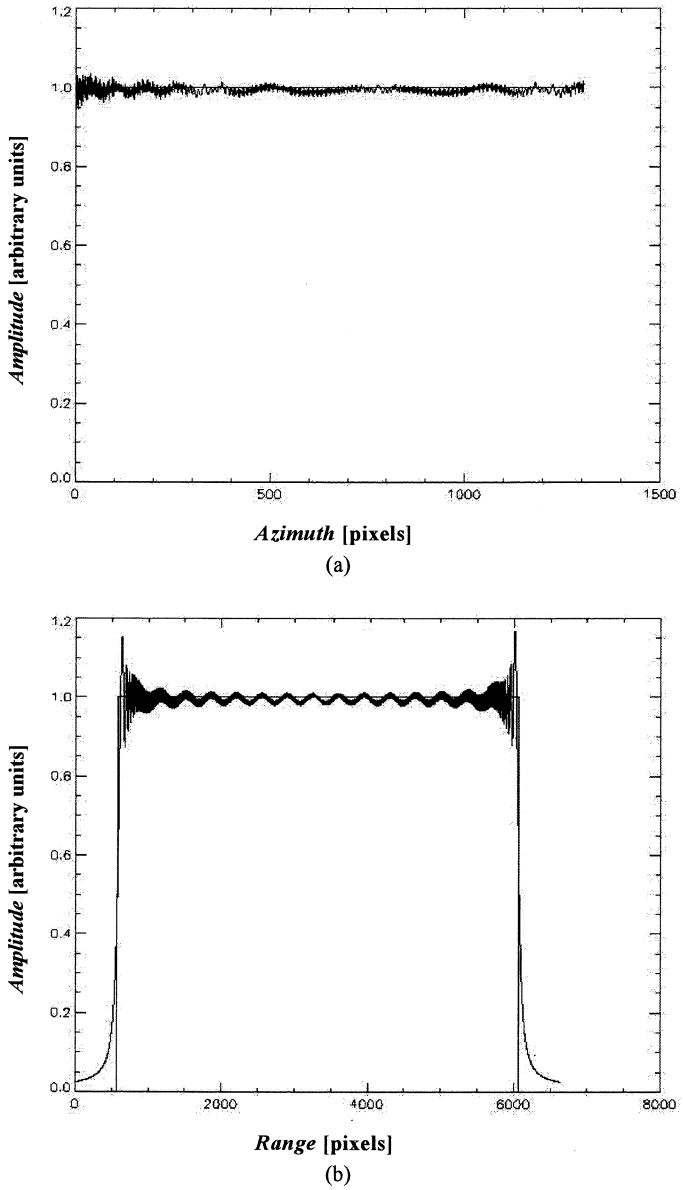

Fig. 5. Amplitudes of the raw signals simulated by using the proposed approach (oscillating curve) and obtained by time-domain simulation (straight line): (a) azimuth cut; (b) range cut. The scattering point is placed near the azimuth border of the illuminated scene.

It is now appropriate to compare the computational complexity of the proposed algorithm to the one of a time-domain direct approach.

The first stage of the simulation (i.e., the generation of the reflectivity map) is the same for both approaches. With regard to the second stage, it is not difficult to verify that the computational complexity of the above described algorithm is

$$N_{\mathrm{FD}} \approx N_x N_r g\left[1+\log_2\left(N_x N_r\right)+\log_2 g\right] \tag{3.1}$$

wherein N_{FD} is the number of complex multiplications, and N_x and N_r are the azimuth and range dimensions (in pixels) of the final spotlight raw signal. Equation (3.1) does not include the cost of the interpolation in the Fourier domain. This cost is negligible if $\Omega \cong 1$ (see Section II); otherwise it may increase by a factor not greater than two, due to the use of chirp scaling (see Section II). In any case, the order of magnitude of N_{FD} does not substantially change with respect to (3.1).

If the spotlight raw signal is evaluated in time domain directly from (2.6), no azimuth oversampling is needed, but the efficiency of FFT codes is not exploited and computational complexity is

$$N_{\mathrm{TD}} \approx \left(N_x N_r\right)^2 \tag{3.2}$$

wherein N_{TD} is the number of complex multiplications in the case of time-domain simulation. Accordingly, by using our Fourier domain approach, processing time is reduced by a factor

$$\frac{N_{\mathrm{TD}}}{N_{\mathrm{FD}}} \approx \frac{N_x N_r}{g\left[1+\log_2\left(N_x N_r\right)+\log_2 g\right]} \tag{3.3}$$

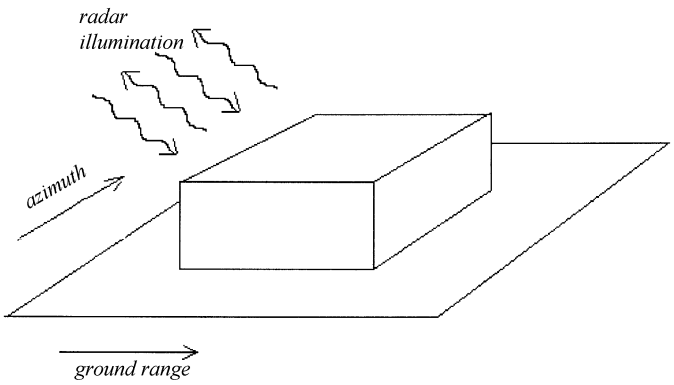

Fig. 6. "Canonical" extended scene. A parallelepiped over a plane.

with respect to a time-domain simulation. For a 4096×4096 spotlight raw signal, if $g = 8$ we obtain a processing time decrease factor of the order of 75 000. This renders spotlight simulation of extended scenes feasible.

IV. Results

In this section, we show and discuss some simulation examples aimed at verifying the effectiveness of the spotlight raw signal simulator and at illustrating some of the potentialities of the simulator.

First of all, we want to verify that the raw signal corresponding to a single scattering point, simulated by using the proposed Fourier domain approach, is in agreement with the one obtained directly from the exact time-domain expression (i.e., (2.6) in which the reflectivity map γ is a Dirac pulse, so that no integration is needed). We consider the system data of a hypothetical spotlight spaceborne sensor, reported in Table I. We first of all consider the raw signal of a point placed in the center of the illuminated scene (i.e., the azimuth coordinate of the point scatterer is $x = 0$). The difference between the phase of the raw signal simulated by using the proposed approach and the phase of the raw signal obtained from (2.6) is reported in the plots of Fig. 2. In particular, in Fig. 2(a) the plot of a cut of this phase difference along the azimuth direction is reported, whereas in Fig. 2(b) the plot of a cut of the same phase difference along the range direction is shown. It can be noted that the absolute value of this phase difference, that can be read as the simulated raw signal phase error, is much smaller than π (in particular, it is always smaller than $\pi/60$), thus leading to negligible effects. We underline that this (negligible) error is due to approximations introduced by the asymptotic evaluation of the SAR system transfer function (see Section II) and is not specific of the spotlight case. Raw signal amplitudes are considered in Fig. 3, where azimuth and range cuts of the amplitude of the raw signals obtained by the Fourier domain approach and by using (2.6) are reported. Only small oscillations around the exact constant value can be noted.

Let us now verify that a correct raw signal simulation is obtained also if the point scatterer is not placed at the center of the scene. Phase and amplitude simulation errors for a point placed near the azimuth border of the illuminated scene are considered in Figs. 4 and 5, respectively, according to the same format of Figs. 2 and 3. It is evident that also in this case a very good agreement is obtained between our simulations and (2.6). Analogous results are obtained for different positions of the scattering point.

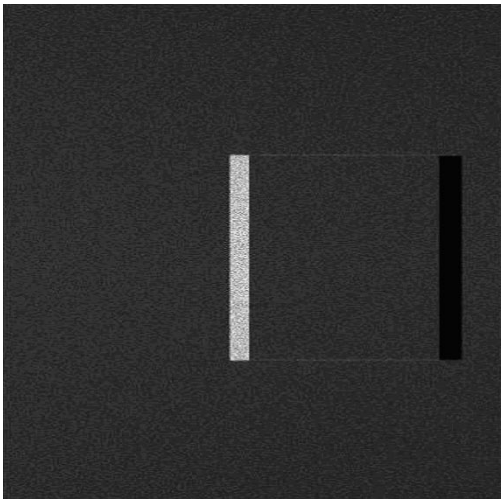

Fig. 7. Image of a parallelepiped over a plane, obtained by processing the simulated spotlight SAR raw signal via a spotlight focusing algorithm. Near range is on the left. A multilook operation over a 8×8 pixel window has been performed on this image, as well as on the image of Fig. 8.

Simulations relevant to extended scenes are now in order. We consider the same system data of Table I and a "canonical" extended scene: a parallelepiped over a flat plane (see Fig. 6). The illuminated scene is about 2.5 km (azimuth)$\times$ 4.2 km (ground range), and spotlight system resolution is 1.85 m (azimuth) $\times$ 3.7 m (ground range). The raw signal size is 1306×6650 pixels. Each raw signal simulation required about 10 min on a Pentium III 866-MHz personal computer. The obtained simulated raw signals have been processed by using an algorithm based on the one of [14], in order to obtain spotlight SAR images. As an example, the image of a parallelepiped over a flat plane[3] is shown in Fig. 7. The bright strip on the left is due to the layover effect in correspondence of the vertical wall in front of the sensor, whereas the black strip on the right is the shadowed area behind the parallelepiped. The horizontal bright lines are due to the fact that in correspondence of the lateral walls of the parallelepiped a very large surface area is included within a single resolution cell. This effect is in large part compensated for by the fact that, on those walls, incidence is at near grazing angle, so that the horizontal lines are much less bright than the layover area corresponding to the vertical wall in front of the sensor.

We underline that we simulate raw signals, not images. This fact can be exploited to test processing algorithms (with an accuracy only limited by simulator approximations shown above); however, other interesting applications are also possible. For instance, our spotlight raw signal simulator can be used to analyze some properties of raw signals and of reflectivity functions. In Fig. 8, we show the image obtained by processing the parallelepiped raw signal by using a Fourier domain efficient stripmap (not spotlight) focusing: the azimuth spectrum folding

[3]Due to our facet approximation of the height profile, "vertical" walls of the parallelepiped are not exactly vertical, but have a (extremely high) slope equal to the height of the parallelepiped divided by the azimuth facet size.

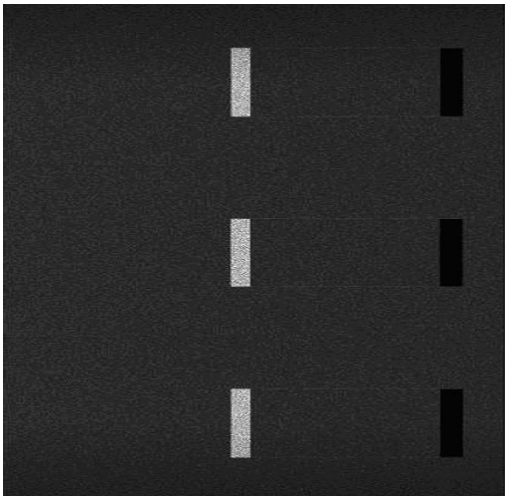

Fig. 8. Image of a parallelepiped over a plane, obtained by processing the simulated spotlight SAR raw signal via a stripmap focusing algorithm. Near range is on the left. Azimuth spectrum folding effect is evident.

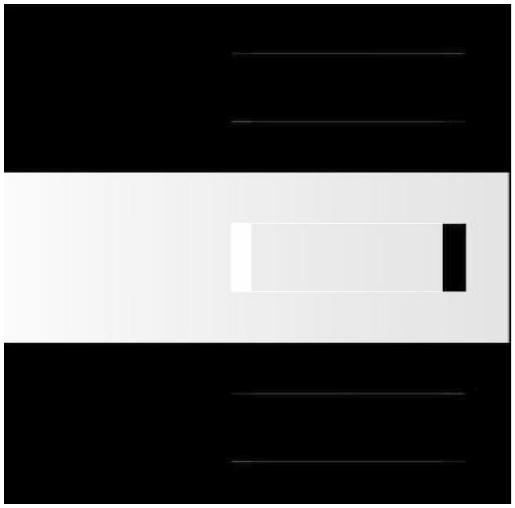

Fig. 9. Nonspeckled image of a parallelepiped over a plane, obtained by processing the simulated spotlight SAR raw signal via a stripmap focusing algorithm. Near range is on the left. Azimuth spectrum folding effect is evident. It is also clear from this image that upper and lower replica are highpass-filtered versions of the image (see text). A nonlinear gray-level scale has been used to produce this image, in order to highlight weak bright lines.

effect, due to the fact that the azimuth raw signal bandwidth is greater than the PRF, causes the appearance of three (i.e., X_1/X) replicas of the imaged scene. This is a well-known effect, already encountered by stripmap processing actual spotlight raw signals, e.g., see [14]. However, images obtained from real raw signals and from simulated raw signals including the speckle effect, do not allow the analyst to immediately realize that each replica corresponds to a different portion of the reflectivity bandwidth. Conversely, by using the spotlight simulator it is possible to generate raw signals not including the speckle effect. The image obtained by stripmap processing the nonspeckled spotlight raw signal of the parallelepiped scene is shown in Fig. 9. In this image, it is evident that the central replica corresponds to the low-frequency part of the reflectivity spectrum, where most of the energy is concentrated (in this nonspeckled case), while upper and lower replicas correspond to the high frequency part of the reflectivity spectrum: in fact, only weak bright lines corresponding to edges perpendicular to the azimuth direction are visible, whereas the areas with constant reflectivity (i.e., the background and the top of the parallelepiped) are filtered out.

V. Conclusion

In this paper, an efficient spotlight SAR raw signal simulator has been presented. It relies on a Fourier domain analysis and allows the use of efficient FFT codes. Accordingly, in the case of the simulation of an extended scene the computational load is strongly reduced with respect to a time-domain simulation and this makes spotlight simulation of extended scenes feasible.

Effectiveness of the simulator has been verified by comparing simulated raw signal corresponding to a single scattering point (placed at different positions in the illuminated scene) to the corresponding available time-domain exact expression.

Spotlight SAR raw signals corresponding to extended canonical scenes have been simulated and then processed by using different focusing algorithms. Results confirm the consistency of the proposed simulation scheme and allow to highlight some interesting properties of the spotlight SAR signals.

References

[1] W. G. Carrara, R. S. Goodman, and R. M. Majewski, *Spotlight Synthetic Aperture Radar: Signal Processing Algorithms*. Norwood, MA: Artech House, 1995.

[2] G. Franceschetti and R. Lanari, *Synthetic Aperture Radar Processing*. Boca Raton, FL: CRC, 1999.

[3] D. C. Munson Jr., J. D. O'Brien, and W. K. Jenkins, "A tomographic formulation of spotlight mode synthetic aperture radar," *Proc. IEEE*, vol. 71, pp. 917–925, 1983.

[4] D. L. Mensa, S. Halevy, and G. Wade, "Coherent doppler tomography for microwave imaging," *Proc. IEEE*, vol. 71, pp. 254–261, 1983.

[5] M. Desai and W. Jenkins, "Convolution backprojection image reconstruction for spotlight mode synthetic aperture radar," *IEEE Trans. Image Processing*, vol. 1, pp. 505–517, May 1992.

[6] J. Mittermayer, A. Moreira, and O. Loffeld, "Spotlight SAR data processing using the frequency scaling algorithm," *IEEE Trans. Geosci. Remote Sensing*, vol. 37, pp. 2198–2214, Sept. 1999.

[7] R. Lanari, M. Tesauro, E. Sansosti, and G. Fornaro, "Spotlight SAR data focusing based on a two-step processing approach," *IEEE Trans. Geosci. Remote Sensing*, vol. 39, pp. 1993–2004, Sept. 2001.

[8] G. Franceschetti, M. Migliaccio, D. Riccio, and G. Schirinzi, "SARAS: A SAR raw signal simulator," *IEEE Trans. Geosci. Remote Sensing*, vol. 30, pp. 110–123, Jan. 1992.

[9] G. Franceschetti, M. Migliaccio, and D. Riccio, "SAR simulation of actual ground sites described in terms of sparse input data," *IEEE Trans. Geosci. Remote Sensing*, vol. 32, pp. 1160–1169, Sept. 1994.

[10] G. Franceschetti, A. Iodice, M. Migliaccio, and D. Riccio, "A novel across-track SAR interferometry simulator," *IEEE Trans. Geosci. Remote Sensing*, vol. 36, pp. 950–962, May 1998.

[11] A. Mori and F. De Vita, "A raw signal simulator for stripmap, spotlight and hybrid mode interferometric SAR on spaceborne platform," in *Proc. SRL Science Mission Meeting: What's next?*, Florence, Italy, 2001.

[12] R. K. Raney, H. Runge, R. Bamler, I. G. Cumming, and F. H. Wong, "Precision SAR processing using chirp scaling," *IEEE Trans. Geosci. Remote Sensing*, vol. 32, pp. 786–799, July 1994.

[13] G. Franceschetti, A. Iodice, S. Maddaluno, and D. Riccio, "Effect of antenna mast motion on X-SAR/SRTM performance," *IEEE Trans. Geosci. Remote Sensing*, vol. 38, pp. 2361–2372, Sept. 2000.

[14] R. Lanari, P. Franceschetti, M. Tesauro, and E. Sansosti, "Spotlight SAR image generation based on strip mode focusing techniques," in *Proc. IGARSS*, Hamburg, Germany, 1999.

Silvia Cimmino was born in Naples, Italy, on June 28, 1976. She graduated summa cum laude in telecommunication engineering from the University of Naples "Federico II," Naples, Italy, in 2001.

She joined the Department of Electronic and Telecommunication Engineering, University of Naples "Federico II," in 2001, where she conducted research on the simulation of SAR raw signals, focusing on SAR systems working in spotlight mode. She is currently with Wide Sensing (WISE), Naples, Italy, where she is performing research for on the simulation of SAR signals and electromagnetic field in urban areas.

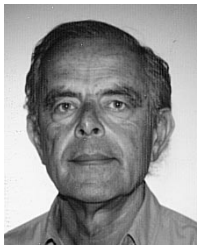

Giorgio Franceschetti (S'60–M'62–SM'85–F'88–LF'01) was born in Italy.

He is currently a Full Professor of electromagnetic wave theory at University of Naples, Naples, Italy, since 1968. He is also an Adjunct Professor at the University of California, Los Angeles (UCLA) and a Distinguished Visiting Scientist at the Jet Propulsion Laboratory, California Institute of Technology (Caltech), Pasadena. He was a Visiting Professor at the University of Illinois, Urbana-Champaign, in 1976 and 1977, and at UCLA in 1980 and 1982. He was a Research Associate at Caltech, in 1981 and 1983, a Visiting Professor at National Somalia University, Mogadishu, Somalia, in 1984, and a Visiting Professor at the University of Santiago de Compostela, Santiago de Compostela, Spain, in 1995. He has published several books and more than 130 refereed papers in the field of applied electromagnetics (reflector antennas, transient phenomena, shielding, nonlinear propagation, and scattering) and, more recently, in the field of SAR data processing and simulation. He has lectured in several summer schools in China, the United Kingdom, Holland, Italy, Spain, Sweden, and the United States.

Dr. Franceschetti was a Fulbright Scholar at Caltech in 1973. He has been the recipient of several national and international awards. He was Director of IRECE, a Research Institute of the Italian National Council of Research (CNR), and member of the board of the Italian Space Agency (ASI).

Antonio Iodice (S'97–M'00) was born in Naples, Italy, on July 4, 1968. He received the laurea degree (with honors) in electronic engineering and the Ph.D. degree in electronic engineering and computer science, both from the Univeristy of Naples, Italy, in 1993 and 1999, respectively.

In 1995, he received a grant from CNR (Italian National Council of Research) to be spent at IRECE (Instituto di Ricerca per 1'Elettromagnetismo e i Componenti Elettronici), Naples, for research in the field of remote sensing. He was with the Department of Electronic and Telecommunication Engineering, University of Naples, from 1996 to 1999, and with Telespazio S.p.A., Rome, Italy, from 1999 to 2000. He is currently a Research Scientist at the Department of Electronic and Telecommunication Engineering, University of Naples. His main research interests are in the field or SAR remote sensing, modeling of electromagnetic scattering from natural surfaces, and SAR interferometry.

Daniele Riccio (M'91–SM'99) was born in Naples, Italy, on April 13, 1962. He received the laurea degree (with honors) in electronic engineering from the University of Naples "Federico II," Naples, Italy, in 1989.

Currently, he is Professor of remote sensing, electromagnetic diagnostics, and guided propagation at the University of Naples "Federico II." He was a Research Scientist at the Istituto di Ricerca sull'Elettromagnetismo e i Componenti Elettronici (IRECE), Italian National Council of Research (CNR), and at the Department of Electronic and Telecommunication Engineering, University of Naples "Federico II." In 1994 and 1995, he was also a Guest Scientist at the DLR High-Frequency Institute, Munich, Germany. His main research activities are in the fields of microwave remote sensing and simulation and modeling of SAR signals relevant to terrestrial and oceanic scenes, as well as in the application of fractal geometry to electromagnetic scattering and remote sensing.

Prof. Riccio has won several fellowships from private and public companies (SIP, Selenia, CNR, CORISTA, and CRATI) for research in the remote sensing field.

Giuseppe Ruello (S'00) was born in Naples, Italy, on February 12, 1975. He received the laurea degree (with honors) in telecommunication engineering, in 1999, and the Ph.D. degree in electronic and telecommunication engineering, in 2003, both from the University of Naples "Federico II," Naples, Italy.

In 2000, he received a grant from the University of Naples to be spent at the Department of Electronic and Telecommunication Engineering for research in the field of remote sensing. In 2000, he won also a grant from University of Rome "La Sapienza," Rome, Italy. In 2002, he was a Visiting Scientist at the Department of Signal Theory and Communications of the Universitat Politecnica de Catalunya, Barcelona, Spain. His main research interests are in the field of SAR remote sensing, modeling of electromagnetic scattering from natural surfaces, and SAR simulation.